Relative total-cross-section measurements for collisions of low-energy electrons (10–25 eV) with N_2 and CO

J. P. Polley
Department of Physics, Rollins College, Winter Park, Florida 32789-4497

T. L. Bailey
Department of Physics, University of Florida, Gainesville, Florida 32611
(Received 3 August 1987)

We report the measurements of the relative total cross sections of collisions between electrons and molecular nitrogen and between electrons and carbon monoxide for incident electron energies in the range 10–25 eV. Through the use of a crossed electron–supersonic-molecular-beam configuration and a phase-lock detection technique we obtain direct measurement of features in the relative total cross section that are approximately 10^{-3} of the total cross section itself. Our measurements confirm that the e^--N_2 collisions exhibit a number of features that can be consistently interpreted with the grandparent model proposed by Sanche and Schultz [Phys. Rev. A **6**, 69 (1972)], and further developed by Brunt, King, and Read [J. Phys. B **11**, 173 (1978)]. The e^--CO collisions are also amenable to this interpretation. We find no evidence of a Feshbach resonance at 15.6 eV and suggest that the Feshbach resonances in the e^--CO system arise from only two grandparent states, as they do in the e^--N_2 system.

I. INTRODUCTION

The study of low-energy electron-molecule collisions has been of interest to physicists for more than six decades. Through the study of such systems we have come to appreciate the complexity of the interactions between an electron and a molecular target, interactions that have not proven to be amenable to detailed theoretical analysis. While there have been a number of calculations[1–4] of the low-energy shape resonances that occur at electron energies of 1.52 eV in e^--CO and of 1.89 eV in e^--N_2 collisions, there are no similarly refined calculations of the features that are found in the scattering cross sections of these two systems at the higher energies of 10–25 eV. Lest this be considered the sniping of disgruntled experimentalists, we hasten to add that the experimental work on these features has been difficult to interpret, as the resonances represent small excursions (10^{-2}–10^{-3}) from the nonresonant scattering cross section. One of the more sensitive methods, which measures the derivative of the transmitted electron current,[5] has been of value in determining if there is or is not a resonance feature in the scattering cross section, but it is difficult to determine the energy and shape of the feature precisely from such measurements. In this paper we describe a method used to measure the relative total scattering cross section (RTSC) that allows us to determine the energies and shapes of features in that cross section that represent resonant scattering. In Sec. II we describe the experiment, in which a modulated supersonic molecular beam and an electron beam collide in a crossed-beam configuration. Section III is a presentation of the relative total cross sections obtained in this study and an analysis of these cross sections using the grandparent model. In Sec. IV we summarize our findings.

II. EXPERIMENT

The apparatus used in these investigations has been described briefly in a previous paper.[6] It is shown schematically in Fig. 1. The molecular target is a supersonic nozzle beam that has a flux of 6.0×10^{14} molecules/cm^2 sec. In the target region, the diameter of the beam is approximately 0.7 cm. The molecular beam is modulated with a mechanical chopper that rotates with a frequency of 57 Hz. A signal from an infrared photogate provides the reference signal for the phase-

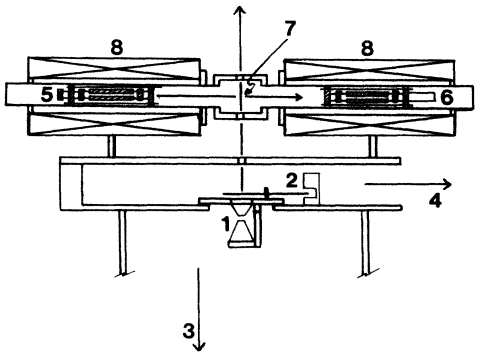

FIG. 1. Cross sectional view of the crossed-beam apparatus. The supersonic beam is produced at the nozzle-skimmer assembly (1) and then modulated by the chopper (2). The pillar to the right of the fan contains the photogate assembly. The gas that is skimmed away is pumped out (3) by a diffusion pump with a pumping speed of 2000 L/sec. The chopper region is itself also pumped through a side port (4). The electron beam is produced by a trochoidal velocity selector (5) and analyzed by a second such selector (6) after traversing the interaction region (7). The magnetic fields for the operation of the trochoidal selectors are provided by solenoids (8) that are aligned with the stainless-steel tube containing the selectors.

sensitive detection (PSD) described below. An advantage that we obtain through the use of a supersonic molecular beam is the elimination of the broadening of the observed features that would result from the thermal motion of the target.[7] At room temperature, the thermal broadening in a nitrogen gas target is approximately 8 meV. In the current work the thermal broadening is of the order of a microvolt.

The kinetic energy of electron beam is defined by a trochoidal velocity selector.[8] After traversing the collision region, the energy of the electron beam is analyzed by a second trochoidal velocity selector. The beam then enters an electron multiplier. The signal from the electron multiplier is processed by a high-voltage isolation preamplifier. The output from the preamplifier is a time-dependent voltage $V(t,E)$ given by

$$V(t,E)=GI_0[1-n(t)Q(E)x] , \quad (1)$$

where G is the input impedance of the electron multiplier and isolation preamplifier, I_0 is the beam current incident on the target, $n(t)$ is the time-varying, spatially averaged density in the target region, $Q(E)$ is the effective cross section for the removal of electrons from the electron beam by the target beam, and x is the length of the electron trajectory in the interaction region.

This signal is then processed by a lock-in amplifier using a signal from the photogate mentioned above as the reference signal. The lock-in removes the dc component from the signal and yields a signal which is directly proportional to $Q(E)$. This $Q(E)$ is very nearly equal to the total cross section $\sigma(E)$ at a given energy E (apart from a constant factor) for the following reasons. First, the second trochoidal analyzer is set to pass electrons of the same kinetic energy as the first analyzer. This prevents any inelastically scattered electrons from passing through the second analyzer. Second, the axial magnetic field provided by the two trochoid solenoids drops from 18.0 mT in the analyzer region to 2.5 mT in the interaction region. Thus a magnetic mirror is formed[9] that prevents electrons that have been elastically scattered by more than a few degrees from entering the second trochoidal velocity selector. This represents a considerable decrease in the acceptance angle for a dual trochoidal electron-impact spectrometer.[10] We find that the effective cross section $Q(E)$, for S-wave scattering, is thus given by

$$Q(E)=\sigma_{\text{in}}(E)+0.97\sigma_{\text{el}}(E) , \quad (2)$$

where $\sigma_{\text{in}}(E)$ is the total inelastic cross section at an energy E, and $\sigma_{\text{el}}(E)$ is the total elastic cross section at the same energy.

The total cross sections are obtained as functions of incident electron energy by repeatedly sweeping the potential applied to the electron spectrometer through a 2.56-V range in 10-meV steps over a period of several hours. The electron beam energy is calibrated at the beginning and end of each run in comparison with the 19.35-eV electron-helium window resonance.[6] The energy distribution of the electron beam is also determined before and after each run using standard retardation procedures. The electron spectrometer usually supplies 8 nA of current with a full width at half maximum of 35 meV.

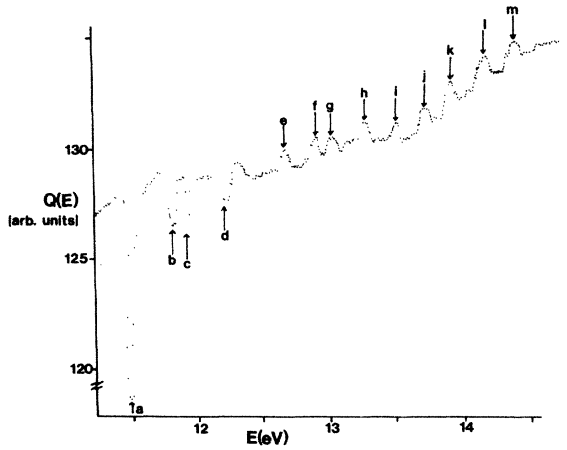

FIG. 2. Relative total cross section of e^--N_2. Feature "a" is shown at half-size. The assignments of the features is given in Table I.

III. RESULTS

A. Nitrogen

The effective cross section $Q(E)$ is plotted as a function of energy in Fig. 2. Arrows indicate the location of the centers of the features, whose values are listed in Table I. The presence of many of these features has been noted before[5,11–15] in electron-molecule collision experiments, but the present work shows the shape and width of these features. These relative total cross sections are also easier to interpret than those from the derivative-current method,[5] having the advantage that the series of vibrational states associated with a particu-

TABLE I. Features in the e^--N_2 relative total scattering cross section. The letters in the feature column refer to the features denoted in Fig. 2. The energy that marks the center of the feature is listed in the energy column. The assignments of the resonances are given in terms of the grandparent model by listing the orbitals of the two Rydberg electrons, then the positive-ion core.

Feature	Energy (eV)	Temporary negative ion
a	11.48	$(3s\sigma_g)^2X^2\Sigma_g^+$, $v=0$
b	11.74	$(3s\sigma_g)^2X^2\Sigma_g^+$, $v=1$
c	11.90	$(3s\sigma_g)(3p\sigma_u)X^2\Sigma_g^+$, $v=0$
d	12.20	$(3s\sigma_g)(3p\Pi_u)X^2\Sigma_g^+$, $v=0$
e	12.64	$(3s\sigma_g)^2A^2\Pi_u$, $v=0$
f	12.87	$(3s\sigma_g)^2A^2\Pi_u$, $v=1$
g	13.00	$(3s\sigma_g)(3p\sigma_u)A^2\Pi_u$, $v=0$
h	13.23	$(3s\sigma_g)(3p\sigma_u)A^2\Pi_u$, $v=1$
i	13.46	$(3s\sigma_g)(3p\sigma_u)A^2\Pi_u$, $v=2$
j	13.70	$(3s\sigma_g)(3p\sigma_u)A^2\Pi_u$, $v=3$
k	13.88	$(3p\sigma_u)^2A^2\Pi_u$, $v=0$
l	14.12	$(3p\sigma_u)^2A^2\Pi_u$, $v=1$
m	14.36	$(3p\sigma_u)^2A^2\Pi_u$, $v=2$

lar grandparent state may be identified more readily.

The two grandparent states which contribute to Feshbach resonances in e^--N_2 collisions are $X^2\Sigma_g^+$ and $A^2\Pi_u$. The first state gives rise to the four features noted between 11.48 and 12.20 eV. These assignments agree with those of (Brunt, King, and Read) BKR. The second state gives rise to three vibrational series, as noted in Table I, the first two of which agree with BKR, while we find that the $(3p\sigma_u)^2$ series begins at 13.88 eV, and not 14.134 eV as they claim. We have also observed the large broad shape resonance that peaks at 22.5 eV, a result that is in good agreement with measurements of the absolute total cross section.[16]

B. Carbon monoxide

The features in e^--CO relative total cross section between 10 and 25 eV are listed in Table II with our assignments of those features. The cross section as a function of energy is displayed in Fig. 3. We have found that the Feshbach resonances in e^--CO collisions involve only two grandparent states $X^2\Sigma^+$ and $A^2\Pi$, and that there is no feature corresponding to the $B^2\Sigma^+$ state. We have also found that the feature at 10.42 eV may be assigned to the $(3s\sigma)$ $(3p\sigma)$ Rydberg electron configuration, an assignment that establishes a close correspondence between the four features seen in the e^--N_2 cross section between 11.48 and 12.20 eV and the four features seen in the e^--CO cross section between 10.04 and 10.72 eV.

The next two features in the e^--CO cross section are more difficult to assign, and we propose that they are core-excited shape resonances. They correspond to no state with a $X^2\Sigma^+$ grandparent, and are too low in energy to have an $A^2\Pi$ grandparent. It seems likely that the first resonance with an $A^2\Pi$ grandparent is found at 12.58 eV. The feature at 12.78 eV is probably the first vibrationally excited state of the $(3s\sigma)^2A^2\Pi$ temporary negative ion, as the vibrational spacing for the $A^2\Pi$ configuration of CO^+ is 190 meV.

TABLE II. Features in the e^--CO relative total cross section. The letters in the feature column refer to the features denoted in Fig. 3. The energy that marks the center of the feature is listed in the energy column. The assignments of the resonances are given in terms of the grandparent model by listing the orbitals of the two Rydberg electrons, then the positive-ion core. The exceptions are the "e" and "f" features, which do not correspond to a possible temporary negative ion, and which are probably core-excited shape resonances.

Feature	Energy (eV)	Temporary negative ion
a	10.04	$(3s\sigma)^2X^2\Sigma^+$, $v=0$
b	10.27	$(3s\sigma)^2X^2\Sigma^+$, $v=1$
c	10.42	$(3s\sigma)(3p\sigma)X^2\Sigma^+$, $v=0$
d	10.72	$(3s\sigma)(3p\Pi)X^2\Sigma^+$, $v=0$
e	11.24	core-excited shape
f	12.18	core-excited shape
g	12.58	$(3s\sigma)^2A^2\Pi_i$, $v=0$
h	12.78	$(3s\sigma)^2A^2\Pi_i$, $v=1$
i	13.98	$(3p\sigma)^2A^2\Pi_i$, $v=0$
j	14.18	$(3p\sigma)^2A^2\Pi_i$, $v=1$
k	14.38	$(3p\sigma)^2A^2\Pi_i$, $v=2$
l	14.56	$(3p\sigma)^2A^2\Pi_i$, $v=3$

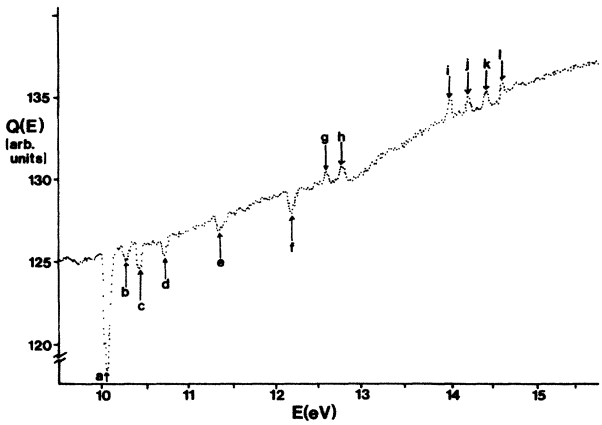

FIG. 3. Relative total cross section of e^--CO. Feature "a" is shown at half-size. The assignments of the features is given in Table II.

We come to another vibrational series beginning at 13.98 eV. The series continues with three vibrationally excited states at 14.18, 14.38, and 14.56 eV, corresponding to $v=1$, 2, and 3, respectively. We find no state corresponding to a $(3s\sigma)$ $(3p\sigma)$ $A^2\Pi$ temporary negative ion, although one is expected at approximately 13 eV. We find no evidence of the feature at 15.6 eV reported by BKR[12] that they interpret as a Feshbach resonance with a $B^2\Sigma^+$ grandparent state.

There is one last feature to comment on, which is the broad shape resonance that is centered at 19.5 eV. We have found no structure either in this shape resonance or in the similar feature in the e^--N_2 cross section. This lack of structure is consistent with the resonant continuum model proposed by Dehmar *et al.*[17] This is in contrast to the observations of Pavlovic *et al.*,[18] who did see structures in the e^--N_2 cross section in this energy region, and in agreement with the observations of Tronc, Azria, and LeCoat,[19] who failed to observe any such features in the e^--CO cross section. The greater energy resolution of the present work confirms the interpretation of these broad features as shape resonances that arise from vibrational excitation of the ground electronic state.[17]

IV. CONCLUSION

We have developed a new method for observing features in the relative total cross section for electron-molecule scattering. This method, which uses dual trochoidal velocity selectors to define and analyze the energy of the electron beam and a supersonic molecular beam as a target, allows us to determine features that represent changes of 10^{-3} in the RTCS. We have used this method to locate a number of features in the RTCS of e^--N_2 and e^--CO scattering, and have been able to assign them to the formation of temporary negative ions using the BKR model. We find that nearly all of the features in the two RTCS studies are consistent with this

model. We have also observed the continuum shape resonances in these RTCS, and find no evidence of vibrational structure in them. The width of these shape resonances, about 7–8 eV, indicates that these resonant states are short lived ($t \simeq 10^{-15}$ sec), compared to the Feshbach resonances, which are much narrower, with widths of 5–50 meV.

We have found that all Feshbach resonances in these two systems arise from two grandparent states; in e^--N_2, the grandparents are $X^2\Sigma_g^+$ and $A^2\Pi_u$, in e^--CO, the grandparents are $X^2\Sigma^+ A^2\Pi$. We found no evidence for a third Feshbach resonance in e^--CO arising from a $B^2\Sigma^+$ grandparent.

[1]A. Herzenberg, J. Phys. B **1**, 548 (1968).
[2]B. T. Birtwhistle and A. Herzenberg, J. Phys. B **4**, 53 (1971).
[3]B. I. Schneider and L. A. Collins, Phys. Rev. A **28**, 166 (1983).
[4]C. F. Wong and J. C. Light, Phys. Rev. A **30**, 2264 (1984).
[5]L. Sanche and G. J. Schulz, Phys. Rev. A **6**, 69 (1972).
[6]J. P. Polley and T. L. Bailey, J. Chem. Phys. **83**, 4276 (1985).
[7]T. L. Bailey and J. M. Mullen, Int. J. Mass Spectrom. Ion Phys. **18**, 339 (1975).
[8]A. Stamatovic and G. J. Schulz, Rev. Sci. Instrum. **38**, 1524 (1968).
[9]J. D. Jackson, *Classical Electrodynamics,* 2nd ed. (Wiley, New York, 1975), pp. 591 and 592.
[10]W. C. Tam and S. F. Wong, Rev. Sci. Instrum. **50**, 302 (1979).
[11]J. Mazeau, F. Grestau, G. Joyez, J. Reinhardt, and R. I. Hall, J. Phys. B **5**, 1890 (1972).
[12]J. N. H. Brunt, G. C. King, and F. H. Read, J. Phys. B **11**, 173 (1978).
[13]N. Swanson, R. J. Celotta, C. E. Kuyatt, and J. W. Cooper, J. Chem. Phys. **62**, 4880 (1975).
[14]J. Comer and F. H. Read, J. Phys. B **4**, 1678 (1971).
[15]A. Huetz, I. Cadez, F. Gresteau, R. I. Hall, and J. Mazeau, Phys. Rev. A **21**, 622 (1980).
[16]R. E. Kennerly, Phys. Rev. A **21**, 1876 (1980).
[17]J. L. Dehmar, J. Siegel, J. Welch, and D. Dill, Phys. Rev. A **21**, 101 (1980).
[18]Z. Pavlovic, M. J. W. Boness, A. Herzenberg, and G. J. Schulz, Phys. Rev. A **6**, 676 (1972).
[19]M. Tronc, R. Azria, and Y. LeCoat, J. Phys. B **13**, 2327 (1980).